Estimation of High-Frequency Oscillation's Magnitude and Frequency based on Multi-tone FIR Filter

Lei Chen, *Member, IEEE,* Xiaorong Xie, *Senior Member, IEEE,* Mingshu Song, Yongguang Li, and Yanjun Zhang

***Abstract*—Recently, several high-frequency oscillation (HFO) events have occurred, and have introduced a serious threat to power system stability. It is significant to estimate HFO magnitude and frequency in a fast and accurate way for HFO early warning and mitigation. This paper designs a novel finite impulse response (FIR) filter that is formed by several weighted window function-based FIR filters with different center frequencies, and is named the multi-tone FIR (MTFIR) filter. The frequency error introduced by the MTFIR filter is analyzed, and optimal MTFIR filter parameters are accordingly selected to achieve the smallest frequency error. Performance tests show that the proposed MTFIR filter estimator is more accurate than the conventional FIR filter, the interpolated discrete Fourier transform, and the P-class harmonic phasor estimator in HFO magnitude and frequency estimation. The response time of the proposed estimator is shorter than 20 ms, which meets the IEEE/IEC standard requirement on protection applications.**

***Index Terms*—High-frequency oscillation (HFO), multi-tone finite impulse response (FIR) filter, oscillation frequency estimation, oscillation magnitude estimation, HFO mitigation.**

I. Introduction

IN RECENT years, several high-frequency oscillation (HFO) events have occurred across the world. For example, in 2013, real HFO events have occurred in German's BorWin1 project, and the oscillation frequency were mostly within 250∼350 Hz [1]. Also, real HFO events have been observed in the France-Spanish INELFE project and China's LuXi project, and the oscillation frequencies are around 1700 Hz [2] and 1272 Hz [3], [4], respectively. [5] also shows that there may exist HFO risk with frequency at 788 Hz in the interconnected system where a wind farm connects to a high-voltage DC (HVDC) system. The HFO frequency can be within a wide range from a few hundred Hz to a few kHz. As these HFO events have brought a serious threat to power system stability, it is significant to estimate the HFO magnitude and frequency in real-time to warn operators as soon as possible and provide key information for HFO mitigation filter design [6].

It should be also noted that the custom high-voltage power transformers may be not able to accurately capture small HFO voltage variations. In contrast, the giant magnetoresistance effect-based current sensor has high accuracy at wide frequency and magnitude ranges [7]. Due to its low price, it is realistic to use current for HFO magnitude and frequency estimation, while the current will introduce harmonic interferences.

As the HFO parameter estimates are used for protection applications, it is required that the estimator should have fast response and low latency. In the IEEE/IEC synchrophasor measurement standard, the reference estimator for P-class phasor measurement units (PMUs) is 2-cycle-long [8]. When using such a short window or even shorter window for the estimation of HFO parameters, the key challenge is the interference from the fundamental and harmonic components.

In literature, few papers have directly addressed the topic of HFO parameter estimation. However, many papers have addressed the topic of low-frequency oscillation (LFO) parameter estimation and subsynchronous oscillation (SSO) parameter estimation. The Matrix Pencil [9] and the estimation of signal parameters via rotational invariance technique (ESPRIT) [10] are usually used for LFO parameter estimation. However, because the sampling frequency of the HFO signal is very high, the computation time will be very long if these methods are also used in HFO parameter estimation. For SSO parameter estimation, there are two kinds of estimators. One is based on the PMU synchrophasor measurements [11]–[13] and the other one is directly based on the sampled signal [14]–[17]. For the former kind, they generally derive the relationship between the SSO parameters and the synchrophasor measurements, and then estimate the SSO parameters based on the relationship. Unfortunately, the maximum PMU reporting rate is only 100 fps, and the synchrophasor measurements can only be used for the parameter estimation of the signal component within 50 Hz, but cannot be used for HFO parameter estimation. On the other side, the iterative Taylor Fourier model [14], the discrete Fourier transform (DFT) [15], the extended Kalman filter [16], and the synchronized waveform-based method [17] were proposed to use the sampled current signal for SSO parameter estimation. However, [14] and [15] use 8-cycle-long or even longer window to detect SSO components, which will make the response time and latency too long. In addition, [16] and [17] will work well when there is no fundamental frequency deviation, or these two methods will have large errors.

Theoretically, interharmonic or harmonic parameter estimators can be also used for HFO magnitude and frequency

This work is supported by State Grid Corporation of China (5108-202136053A-0-0-00). (*Corresponding author: Xiaorong Xie*)

Lei Chen and Xiaorong Xie are with the State Key Lab. of Power Systems, Department of Electrical Engineering, Tsinghua University, Beijing, 100084, China (e-mail: chenleithu@hotmail.com, xiexr@tsinghua.edu.cn).

Mingshu Song, Yongguang Li, and Yanjun Zhang are with State Grid Xinjiang Electric Power Company, Urumchi 830063, Xinjiang Uygur Autonomous Region, China.

estimation. For example, the interpolated DFT (IpDFT) [18], [19] is widely used for interharmonic parameter estimation due to its simplicity and low computation burden. A P-class harmonic phasor estimator (P-HPE) with a fast response was also introduced in [20]. When there is a large fundamental frequency deviation, the interference from the fundamental component will make the estimation errors of these methods very large, especially when the window length is very short. Also, a flat-top filter-based harmonic phasor estimator by using a 13-fundamental-cycle window was introduced in [21], which has a slow response due to the long window length. Other interharmonic or harmonic analysis tools are carefully reviewed in [22]. However, few of them have addressed the topic of interharmonic parameter estimation in a manner of fast response, low computation burden, and great suppression of the fundamental and harmonic interferences.

Finite impulse response (FIR) filters are very easy to be implemented in hardware chips. Also, the requirements of fast response and low computation burden can be satisfied by designing a low-order filter. Thus, it is preferred to use this kind of filter to estimate the HFO magnitude and frequency. The filter's performances for HFO parameter estimation depend on the stopband and transition band performances, which relate to the performances of fundamental and harmonic interferences mitigation. A window function is usually used to modify the performances of the passband, transition band, and stopband of the filters [23]. Several windows are designed by maximizing the main lobe width or sidelobe level, such as the Kaiser window [23]. However, these metrics do not necessarily mean that the attenuation at a specific frequency band, e.g., fundamental and harmonic frequency bands, is the optimal one. A solution to this problem is introducing a new adjustable parameter in the filter design for the modification of the performances at specific frequency band. One may note that including harmonic components in the signal model can also introduce high attenuation at a specific frequency. However, when the window length is very short, harmonic components closed to the HFO component cannot be included in the signal model, or a singular solution to the FIR filter will be introduced.

To address this problem, we propose a multi-tone FIR (MTFIR) filter, which is designed as the sum of several weighted FIR filters with different center frequencies. The frequency deviation between the center frequencies can be modified to improve the attenuation at specific frequency bands. Based on the proposed MTFIR filter, the contributions of this paper are listed as follows:

- The MTFIR filter is designed for HFO parameter estimation. To the best knowledge of the authors, this is the first paper that designs such a novel filter for HFO parameter estimation.
- The frequency error introduced the MTFIR filter is analyzed, and then optimal MTFIR parameters are selected based on the analysis results to achieve the smallest frequency error.
- Simulation tests show that the proposed estimator has higher accuracy than the conventional FIR filter, the IpDFT, and the P-HPE in HFO magnitude and frequency estimation. The response times of the proposed estimator are always shorter than 20 ms.

II. A Brief Introduction of the HFO and the Mitigation Technique

After analyzing the occurred HFO events, it can be observed that they generally happened in the voltage source converter-HVDC (VSC-HVDC) transmission systems. In these events, an MMC's equivalent resistance may be negative at high frequency due to the latencies in the control loops [3], [24]. This is the key reason that the VSC-HVDC transmission system may be unstable. The equivalent reactance of the MMC at high frequencies is always larger than 0 Ω [24]. Accordingly, the equivalent reactance of the AC transmission lines can be negative at high frequency. When the absolute reactance of the MMC is equal to that of the transmission lines, an HFO event may happen when the equivalent resistance of the system is negative.

There are mainly three kinds of HFO mitigation method: the physical filter-based method [3], the digital second-order low pass filter (LPF)-based method [4], and the digital adaptive notch filter (ANF)-based method [6]. Because the HFO frequency can be varied in a wide range from 300 Hz to 1800 Hz, the physical filter and the digital LPF filter cannot mitigate the HFO in a wide frequency band well. Alternatively, the third method can deal with this problem well. A notch filter is embedded into the voltage feed-forward loop of the VSC. The filter's parameter of the ANF is adaptively changed according to the estimated HFO frequency. The performances of this method have been validated in [6]. Thus, estimation of the HFO frequency is very useful in HFO mitigation.

III. Proposed MTFIR filter

A. Introduction of the Window Function-based FIR Filter

A window function-based FIR filter for signal parameter estimation can be given by:

$$\psi[n] = w[n]e^{j2\pi f_c n T_\mathrm{s}} \quad n \in [-N, N] \tag{1}$$

where $2N+1$ is the window length; f_c is the center frequency of the FIR filter; $w[n]$ is a window function; $T_\mathrm{s} = n/f_\mathrm{s}$ is the sampling interval, and f_s is the sampling frequency. Consider a discrete current signal containing HFO component as follows:

$$\begin{aligned} s[n] &= \sqrt{2}[a_1\cos(2\pi f_1 n T_\mathrm{s} + \theta_1) + a_i\cos(2\pi f_i n T_\mathrm{s} + \theta_i) \\ &\quad + a_h\cos(2\pi h f_1 n T_\mathrm{s} + \theta_h)] \\ &= \frac{\sqrt{2}}{2}[p_1 e^{2\pi f_1 n T_\mathrm{s}} + p_1^* e^{-2\pi f_1 n T_\mathrm{s}}] \\ &\quad + \frac{\sqrt{2}}{2}[p_i e^{2\pi f_i n T_\mathrm{s}} + p_i^* e^{-2\pi f_i n T_\mathrm{s}}] \\ &\quad + \frac{\sqrt{2}}{2}[p_h e^{2\pi h f_1 n T_\mathrm{s}} + p_h^* e^{-2\pi h f_1 n T_\mathrm{s}}] \quad n \in [-N, N] \end{aligned} \tag{2}$$

where a_1, a_h, and a_i are the magnitudes of the fundamental, hth harmonic and HFO components, respectively; f_1, θ_h, and f_i are the fundamental and HFO frequencies, respectively; θ_1 and θ_i are the phases of the fundamental, hth harmonic, and

This article has been accepted for publication in a future issue of this journal, but has not been fully edited. Content may change prior to final publication. Citation information: DOI 10.1109/TPWRS.2022.3155630, IEEE Transactions on Power Systems

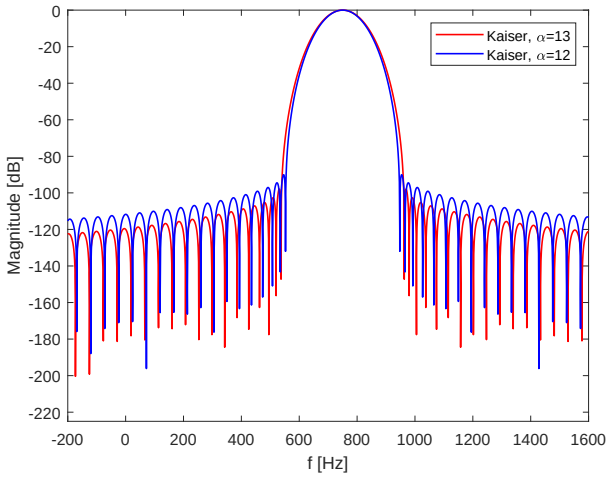

Fig. 1. Normalized magnitude responses of the Kaiser window-based FIR filter with different parameters α. The window length is 1 fundamental cycles long; $f_c = 750$ Hz.

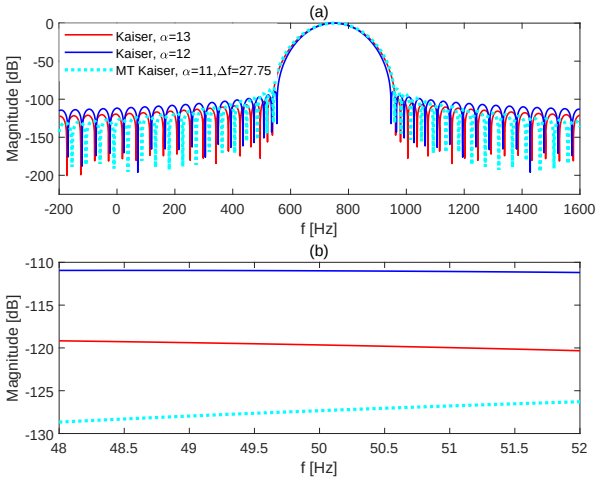

Fig. 2. Normalized magnitude responses of the FIR and MTFIR filters, (a) -200-1600Hz; (b) 48-52 Hz. The window length is 1 fundamental cycle long; $f_c = 750$ Hz; K=1; y_{-1}=y_1=3; y_0=1.

HFO components, respectively; $p_1 = a_1 e^{\theta_1}$, $p_h = a_h e^{\theta_h}$, and $p_i = a_i e^{\theta_i}$ are the corresponding phasors of the fundamental, hth harmonic, and HFO components, respectively; and * represents the conjugate operator. Please note that although the HFO magnitude may be time-variant, it is assumed as constant in a short observation window.

The HFO phasor can be estimated by using the FIR filter:

$$p[0] = \frac{1}{\sum_{n=-N}^{N} w[n]} \sum_{n=-N}^{N} s[n] * \psi[-n] \tag{3}$$

Then the HFO frequency can be estimated by:

$$\tilde{f}_i = \frac{\angle p[1] - \angle p[0]}{2\pi T_s} \tag{4}$$

The HFO frequency may deviate from f_c, and then passband ripples may exist. To address this condition, the HFO magnitude $|p[0]|$ can be compensated by

$$\tilde{a}_i[0] = \frac{|p[0]|}{|H(\tilde{f}_i)|} \tag{5}$$

where

$$H(f) = \sum_{n=-N}^{N} \psi[n] e^{-j2\pi f n T_s} \tag{6}$$

is the frequency response of the FIR filter. In [23], the Kaiser window was especially recommended for harmonic analysis, and can be given by [23]

$$w[n] = \frac{I_0(\alpha\sqrt{1-(\frac{n}{N})^2})}{I_0(\alpha)} \quad n \in [-N, N] \tag{7}$$

where

$$I_0(x) = \sum_{k=0}^{\infty} [\frac{(\frac{x}{2})^k}{k!}]^2 \tag{8}$$

The frequency response of the FIR filter is

$$H(f) = \frac{2N}{I_0(\alpha)} \frac{\sinh(\sqrt{\alpha^2 - (2\pi N(f-f_c))^2})}{\sqrt{\alpha^2 - (2\pi N(f-f_c))^2}} \tag{9}$$

The performances of the window function-based FIR filter can be modified only by changing the value of α, which can be seen from Fig. 1. Improving the stopband attenuation will sacrifice the transition band attenuation. To use a smaller sacrifice of the transition band performance to get the same or better stopband performance at fundamental frequency band, we propose a new FIR filter in next section.

B. Proposed Multi-tone FIR Filter

To achieve the goal mentioned earlier, one way is to introduce another adjustable parameter in the conventional FIR filter. In this regard, we propose a novel FIR filter as follows:

$$\psi_m(t) = \sum_{k=-K}^{K} y_k w[n] e^{j2\pi(f_c + k\Delta f)t} \tag{10}$$

where Δf is an adjustable frequency; $2K$ is the number of the added tones; y_k is the weight for tone k. We can see that there are $2K+1$ tones of FIR filters in the newly designed filter, which is called multi-tone FIR (MTFIR) filter in this paper. Each tone has a different center frequency. After choosing particular values of K and y_k, we can modify Δf and the parameter of $w[n]$ (e.g., α of the Kaiser window) to adjust the frequency response of $\psi_m(t)$ at specific frequency bands. The spectrum of $\psi_m(t)$ is:

$$H_m(f) = \sum_{k=-K}^{K} y_k \Psi(f - k\Delta f) \tag{11}$$

Then the HFO phasor can be estimated by:

$$p_m[0] = \frac{1}{\sum_{k=-K}^{K} \sum_{n=-N}^{N} y_k w[n]} \sum_{n=-N}^{N} s[n] * \psi_m[-n] \tag{12}$$

Then the HFO frequency can be estimated by

$$\tilde{f}_{i,m} = \frac{\angle p_m[1] - \angle p_m[0]}{2\pi T_s} \tag{13}$$

This article has been accepted for publication in a future issue of this journal, but has not been fully edited. Content may change prior to final publication. Citation information: DOI 10.1109/TPWRS.2022.3155630, IEEE Transactions on Power Systems

The HFO magnitude $|p_m[0]|$ is compensated based on the frequency response of the MTFIR, i.e.,

$$\tilde{a}_{i,m}[0] = \frac{|p_m[0]|}{|H_m(\tilde{f}_{i,m})|} \tag{14}$$

In Fig. 2, the magnitude responses of the FIR filter and the MTFIR filter are shown. Generally, the frequency response of the MTFIR filter is the linear combination of the FIR filters, and the added tones overlap the frequency response of the MTFIR filter. By selecting a proper Δf, the MTFIR will remarkably improve the stopband attenuation at the fundamental frequency band (see Fig. 2(b)) with a similar transition band attenuation, which can be seen from the red and cyan lines. In this way, we achieve the goal of designing an MTFIR filter that sacrifices similar transition band performances to get better stopband performances at the specific frequency band. This is very important for fundamental and harmonic interferences mitigation. In addition, parameter selection is very important for the performances of the MTFIR filter. Next, we show a scheme to select the optimal MTFIR parameters (e.g., α and Δf when using Kaiser window).

IV. Optimal Filter Parameter Selection

A. Selection Scheme

In order to find the optimal parameters, we first analyze the frequency error introduced by the MTFIR filter. Then we design an optimization selection scheme based on the analysis results. Please note that because the HFO frequency estimates are very useful for HFO mitigation, this paper analyzes the source of frequency error for MTFIR parameter selection.

Because harmonic interference can be similarly analyzed like the fundamental interference, this paper takes fundamental interference as an example to simplify the analysis. For the signal in (2), when neglecting harmonics, the HFO phasor estimated by the MTFIR filter can be given by:

$$\begin{aligned} p_m[0] = {} & p_1 * H_m(f_1) + p_1^* * H_m(-f_1) \\ & + p_i * H_m(f_i) + p_i^* * H_m(-f_i) \end{aligned} \tag{15}$$

Then the HFO frequency estimate can be given by:

$$\begin{aligned} \tilde{f}_{i,m} &= \frac{\Delta\theta}{2\pi T_\mathrm{s}} = \frac{\angle p_m[1] - \angle p_m[0]}{2\pi T_\mathrm{s}} \\ &= \frac{1}{2\pi T_\mathrm{s}} \angle [p_1 H_m(f_1) E_1 + p_1^* H_m(-f_1) E_1^* \\ &+ p_i H_m(f_i) E_i + p_i^* H_m(-f_i) E_i^*] \\ &- \frac{1}{2\pi T_\mathrm{s}} \angle [p_1 H_m(f_1) + p_1^* H_m(-f_1) \\ &+ p_i H_m(f_i) + p_i^* H_m(-f_i)] \end{aligned} \tag{16}$$

where $\Delta\theta$ is the phase difference between two consecutive HFO phase estimates; $E_1 = e^{j2\pi f_1 T_\mathrm{s}}$; and $E_i = e^{j2\pi f_i T_\mathrm{s}}$. The actual HFO frequency should be calculated by:

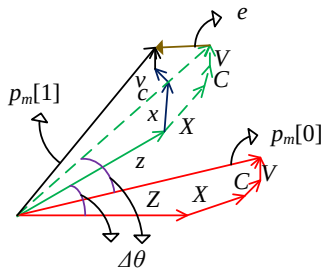

Fig. 3. Visualized presentation of the frequency error source, where $Z = p_i H_m(f_i)$, $X = p_1 H_m(f_1)$, $C = p_1^* H_m(-f_1)$, $V = p_i^* H_m(-f_i)$, $z = p_i H_m(f_i) E_i$, $x = p_1 H_m(f_1) E_1$, $c = p_1^* H_m(-f_1) E_1^*$, and $v = p_i^* H_m(-f_i) E_i^*$. $\Delta\theta = 2\pi f_i T_\mathrm{s}$ is the actual phase difference between two consecutive phasors.

$$\begin{aligned} f_i &= \frac{\angle p_i H_m(f_i) E_i - \angle p_i H_m(f_i)}{2\pi T_\mathrm{s}} \\ &= \frac{1}{2\pi T_\mathrm{s}} \angle [p_i H_m(f_i) E_i + p_1 H_m(f_1) \\ &+ p_1^* H_m(-f_1) + p_i^* H_m(-f_i)] \\ &- \frac{1}{2\pi T_\mathrm{s}} \angle [p_i H_m(f_i) + p_1 H_m(f_1) \\ &+ p_1^* H_m(-f_1) + p_i^* H_m(-f_i)] \end{aligned} \tag{17}$$

By comparing (16) and (17), we can see that the frequency error is mainly related to the angle difference between the term $p_1^* H_m(-f_1) E_1^* + p_i H_m(f_i) E_i + p_i^* H_m(-f_i) E_i^*$ and the term $p_1 H_m(f_1) + p_1^* H_m(-f_1) + p_i^* H_m(-f_i)$ (i.e., $x + c + v$ and $X + C + V$ in figure 3). From Fig. 3, we can see that this angle difference is related to the following term:

$$\begin{aligned} e &= |p_1 H_m(f_1)| E_1 + |p_1^* H_m(-f_1)| E_1^* + |p_i H_m(-f_i)| E_i^* \\ &= a_1 |H_m(f_1)| E_1 + a_1 |H_m(-f_1)| E_1^* + a_i |H_m(-f_i)| E_i^* \end{aligned} \tag{18}$$

Similarly, when considering harmonic interferences, then the angle difference is related to the following term:

$$\begin{aligned} e = {} & a_1 |H_m(f_1)| E_1 + a_1 |H_m(-f_1)| E_1^* + a_i |H_m(-f_i)| E_i^* \\ & + a_h |H_m(h f_1)| E_h + a_h |H_m(-h f_1)| E_h^* \end{aligned} \tag{19}$$

where $E_1 = e^{j2\pi h f_1 T_\mathrm{s}}$. According to the law of cosines, the smaller the magnitude of e is, the smaller such angle difference is. Based on this, we can form an optimization problem to find optimal MTFIR parameters. If the window function is the Kaiser window. Then the optimization problem is

$$\min \quad |e| \tag{20}$$

$$\text{s.t.} \quad \begin{cases} \alpha \in [\alpha_{min}, \alpha_{max}]; \\ \Delta f \in [f_{min}, f_{max}]. \end{cases} \tag{21}$$

where α_{min} and α_{max} are the selected lower and upper bounds of the parameter α of the Kaiser window, respectively; and f_{min} and f_{max} are the selected lower and upper bounds of Δf, respectively. Similarly, the optimal parameter of the

This article has been accepted for publication in a future issue of this journal, but has not been fully edited. Content may change prior to final publication. Citation information: DOI 10.1109/TPWRS.2022.3155630, IEEE Transactions on Power Systems

TABLE I
OPTIMAL PARAMETERS OF THE MTFIR AND THE FIR FILTERS WHEN USING THE KAISER WINDOW.

f_c [Hz]	MTFIR	FIR
{300}	$\alpha = 10.6$, $\Delta f = 21.6$ Hz	$\alpha = 12.6$
{350}	$\alpha = 10.8$, $\Delta f = 22.6$ Hz	$\alpha = 12.2$
{400}	$\alpha = 10.7$, $\Delta f = 24.8$ Hz	$\alpha = 12.4$
{450}	$\alpha = 10.5$, $\Delta f = 24.6$ Hz	$\alpha = 12.2$
{500}	$\alpha = 10.4$, $\Delta f = 26.2$ Hz	$\alpha = 12.4$
{550}	$\alpha = 10.6$, $\Delta f = 26.6$ Hz	$\alpha = 12.4$
{600}	$\alpha = 10.6$, $\Delta f = 27.0$ Hz	$\alpha = 12.4$
{650, 700, 750}	$\alpha = 10.4$, $\Delta f = 27.2$ Hz	$\alpha = 12.4$
{800, 850, 900, ..., 1700}	$\alpha = 10.4$, $\Delta f = 27.2$ Hz	$\alpha = 12.2$

conventional FIR filter can be searched by the following optimization problem:

$$\min \quad |e_{fir}| \tag{22}$$
$$\text{s.t.} \quad \alpha \in [\alpha_{min}, \alpha_{max}]. \tag{23}$$

where

$$e_{fir} = a_1|H(f_1)|E_1 + a_1|H(-f_1)|E_1^* + a_i|H(-f_i)|E_i^* + a_h|H(hf_1)|E_h + a_h|H(-hf_1)|E_h^* \tag{24}$$

is the frequency error source of the conventional FIR filter.

The fundamental frequency may have a deviation in practice. In this regard, when finding the optimal parameters, f_1 can be selected within a frequency band, and each fundamental frequency will result in a different value of $|e|$. The maximum one within all these values should be selected as the representative of $|e|$ in (20). After selecting the window length $2N+1$, the number of the added tones $2K$, the weights y_k of different tones the ratio of the fundamental magnitude to the HFO magnitude a_1/a_i, the considered harmonic components, and the ratio of the fundamental magnitude to the harmonic magnitude a_1/a_h, these two optimization problems can be solved by the enumeration method i.e., the trial and error method, with respect to different center frequencies.

B. Selected Optimal Parameters

In this section, we firstly present general settings in this paper, and then show the corresponding optimal parameters. The sampling frequency is set at 10 kHz, and the added tones $2K$ in the MTFIR filter are set at 2. The weights of different tones are y_{-1}=y_1=3 and y_0=1. The fundamental frequency varies from 48 Hz to 52 Hz. As stated in section I, a window length shorter than 2 fundamental cycles can be used to get a fast response and low latency. In this paper, the window length is set to 1 fundamental cycle long. Because the frequencies of the past HFO events were within (250, 1700] Hz, the center frequency f_c is set from 300 Hz to 1700 Hz in a step of 50 Hz. Two harmonics with frequencies larger and smaller than f_c 200 Hz are considered in the signal model. The harmonic and HFO magnitudes are all set to 1% of the fundamental one. Then the optimal parameters of the MTFIR and the conventional FIR can be searched for different center frequencies, and the corresponding results when using the Kaiser window are shown in TABLE I.

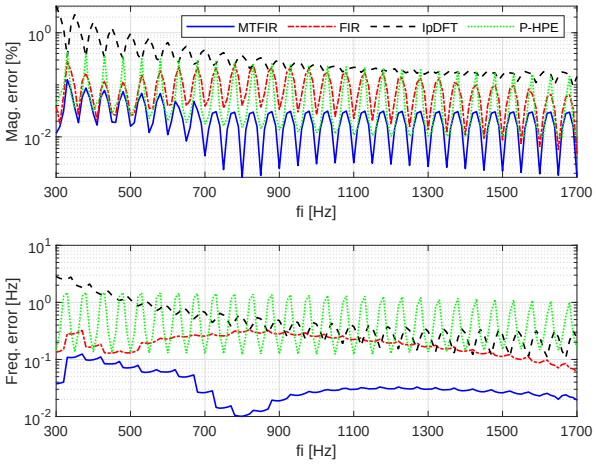

Fig. 4. Magnitude and frequency errors of the MTFIR filter, the conventional FIR filter, the IpDFT, and the P-HPE under various HFO frequencies conditions.

V. SIMULATION TESTS

This section tests the performances of the proposed MTFIR filter under various HFO frequencies, fundamental frequency deviation, harmonic distortion, power swings, noise interference, multiple disturbances, and step change conditions. The conventional FIR filter, the latest P-class harmonic phasor estimator (P-HPE) [20], and the IpDFT [19] are also tested and compared with the proposed estimator. For a fair comparison, all the estimators have the same window length, and the conventional FIR filter and the P-HPE also compensate the estimated magnitude like (14). The Kaiser window is both used in the conventional FIR filter and MTFIR filter. Regarding the IpDFT, the iteration procedure in [19] is not considered in this paper as other estimators do not have iteration procedure as well. Regarding the P-HPE, the decaying dc (DDC) component is not included in the signal model as the key point is the HFO component but not DDC in this paper. Also, the Kaiser window rather than the rectangle window is used to weight the signal model and thus to improve stopband performances. These actions will improve the P-HPE's performance of fundamental and harmonic interference mitigation. The parameter settings of $f_s, f_c, y_k, K, \alpha, \Delta f$ are the same with those in section IV-B, and the window length is 1 fundamental cycle long.

The implementation steps of the proposed estimator are:

- Input signal samples and compute HFO phasors based on (12) at all considered center frequencies (see TABLE I);
- Choose the phasors with the largest magnitude. Then compute HFO frequency using (13) and compensate magnitude using (14).

This article has been accepted for publication in a future issue of this journal, but has not been fully edited. Content may change prior to final publication. Citation information: DOI 10.1109/TPWRS.2022.3155630, IEEE Transactions on Power Systems

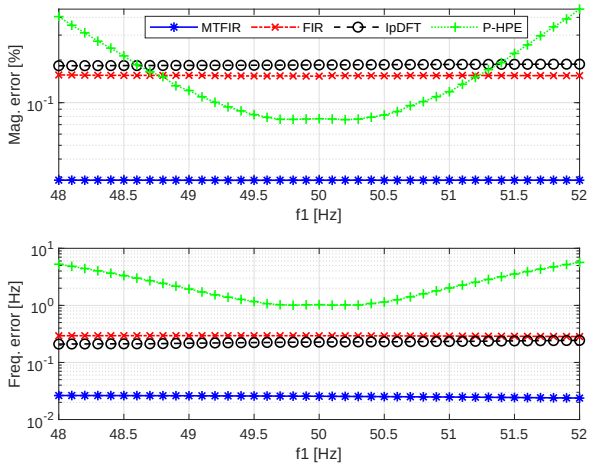

Fig. 5. Magnitude and frequency errors of the MTFIR filter, the conventional FIR filter, the IpDFT, and the P-HPE under fundamental frequency deviation conditions.

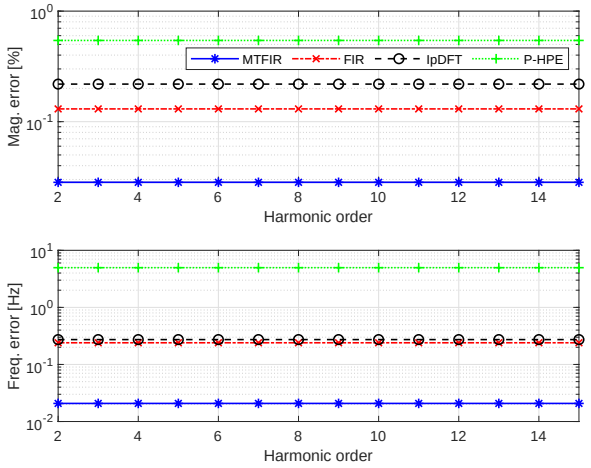

Fig. 6. Magnitude and frequency errors of the MTFIR filter, the conventional FIR filter, the IpDFT, and the P-HPE under harmonic distortion conditions.

A. Various HFO Frequencies

As stated in section I, HFO frequency can vary within a wide frequency band. In this section, the signal in (25) is used for the test, where f_i varies from 300 Hz to 1700 Hz in a step of 10 Hz, f_1 is set at 50 Hz, and $\sigma = 1$ is the damping factor.

$$s(t) = \cos(2\pi f_1 t) + 0.01 e^{\sigma t} \cos(2\pi f_i t + \frac{\pi}{3}) \quad t \in [0, 1] \quad (25)$$

The magnitude and frequency errors of the four estimators under various HFO frequencies conditions are shown in Fig. 4. Even though the HFO frequency may be different, the proposed MTFIR filter is always more accurate than the conventional FIR filter, the IpDFT, and the P-HPE in HFO magnitude and frequency estimations. For example, the overall maximum magnitude errors of the MTFIR filter, the conventional FIR filter, the IpDFT, and the P-HPE are 0.13%, 0.28%, 3.25%, and 0.43%, respectively. The overall maximum frequency errors of these four estimators are 0.12 Hz, 0.33 Hz, 2.84 Hz, and 1.49 Hz, respectively. We can see that *over half* of the conventional FIR filter's magnitude and frequency errors are avoided. When the HFO frequency is around 400-500 Hz, the accuracy improvements of the MTFIR filter are smaller than the results at other frequencies. However, the magnitude accuracy improvements are still larger than 19%, which is still appreciable. The maximum magnitude and frequency errors of the IpDFT are very large when the HFO frequency is close to f_1. This is because the DFT cannot mitigate the fundamental interference well in such a case. In comparison, because the selected optimal parameters let the MTFIR filter have higher stopband attenuation around fundamental frequency than the other three estimators, the proposed estimator can mitigate the fundamental interference well.

B. Fundamental Frequency Deviation

The fundamental frequency may have a deviation from the nominal one. According to the IEEE/IEC Standard [8], the fundamental frequency f_1 in signal (25) is set from 48 to 52 Hz in a step of 0.1 Hz. The HFO frequency is set at 970 Hz, and σ is still set to 1.

In Fig. 5, the magnitude frequency errors of the four estimators under fundamental frequency deviation conditions are shown. We can see that even though there is a 2-Hz fundamental frequency deviation, the magnitude and frequency errors of the MTFIR filter have few changes with respect to the errors when $f_1 = 50$ Hz. Also, they are still much lower than the errors of the other three estimators. This shows that the proposed estimator has good stopband attenuation performances around the fundamental frequency.

C. Harmonic Distortion

Harmonics can exist in current signals when an HFO event occurs. We add 1% harmonic with an order from the 2nd to the 15th in signal (25). The fundamental frequency is 50 Hz, and other parameters (σ, f_i) are the same as those in section V-B.

The corresponding results of the four estimators are shown in Fig. 6. We can see that even though there are harmonic interferences, the magnitude and frequency errors of the MTFIR filter have few changes. The advantages of the MTFIR filter over the other three estimators are still remarkable. The reason can be divided into two folders. First, because the errors caused by the harmonics are considered in the selection of the optimal parameters. As a result, the MTFIR filter can mitigate both the harmonic and fundamental interferences well. Second, although the harmonic frequency may be very close to the center frequency of the MTFIR filter, the harmonic magnitude is much smaller than the fundamental one, and the harmonics have few impacts on the estimation errors of the MTFIR filter.

D. Power Swings

When an HFO event occurs, there may also exist power swings. This section tests the performances of the proposed estimator under such a condition. According to the IEEE/IEC standard [8], the test signal with amplitude modulation (AM)

This article has been accepted for publication in a future issue of this journal, but has not been fully edited. Content may change prior to final publication. Citation information: DOI 10.1109/TPWRS.2022.3155630, IEEE Transactions on Power Systems

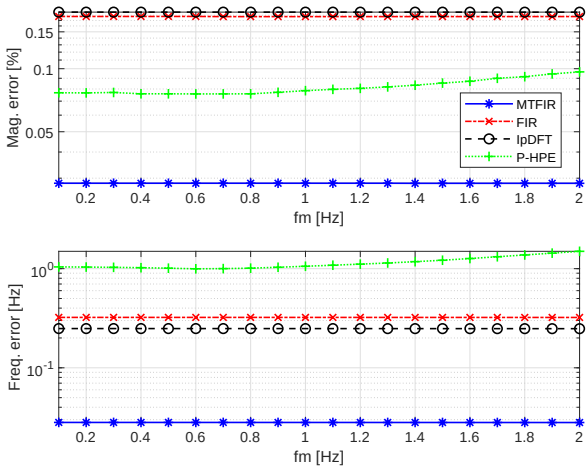

Fig. 7. Magnitude and frequency errors returned by the MTFIR filter, the conventional FIR filter, the IpDFT, and the P-HPE under power swing conditions.

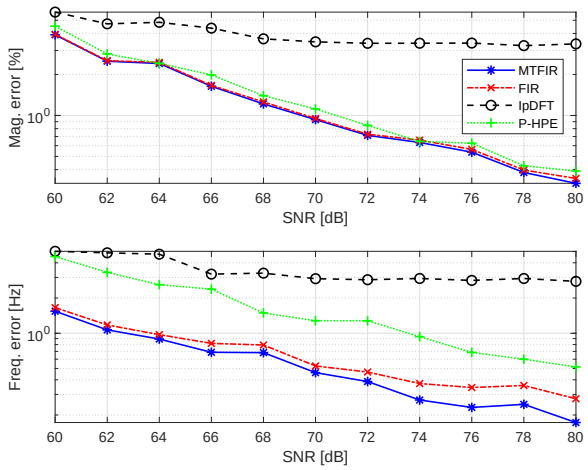

Fig. 8. Magnitude and frequency errors returned by the MTFIR filter, the conventional FIR filter, the IpDFT, and the P-HPE under noise interference conditions.

and phase modulation (PM) is shown in (26), where f_m is the modulation frequency, and is set from 0.1 Hz to 2 Hz in a step of 0.1 Hz. Other parameters (f_1, σ, f_i) are the same as those in section V-A.

$$s(t)= (1+0.1\cos(2\pi f_m t))\cos(2\pi f_1 t + 0.1\cos(2\pi f_m t - \pi)) \\ +0.01e^{\sigma t}\cos(2\pi f_i t + \frac{\pi}{3}) \quad t \in [0,1] \tag{26}$$

The corresponding results of the four estimators are shown in Fig. 7. We can see that only the P-HPE's estimation errors have some changes when the modulation frequency increases, and the errors of the other three estimators have few changes. Also, the MTFIR filter is more accurate than the other three estimators. To justify this, from Fig. 2(b), we can see that the MTFIR filter has similar performances from 48 Hz to 52 Hz, and thus the MTFIR filter can significantly mitigate the interference caused by the power swings.

E. White Noise

White noise can exist in current signals. In this section, white noise with a signal-to-noise ratio (SNR) from 60 dB to 80 dB in a step of 2 dB is added to the signal in (25). The fundamental frequency is 50 Hz; f_i is set to 300 Hz; and σ is set to 1.

The corresponding results of the four estimators are shown in Fig. 8. In general, with the increase of SNR, the magnitude and frequency errors of the four methods will all decrease. Also, the MTFIR filter is still more accurate than the conventional filter, the IpDFT, and the P-HPE in both two parameters' estimation. When the SNR is close to 60 dB, the magnitude and frequency errors returned by the MTFIR filter and the conventional FIR filter are very close, especially for the magnitude estimation. This is because the estimation errors caused by the wideband noise interference are more significant in such a case, and the advantage of the MTFIR filter over the FIR filter in fundamental interference mitigation is comparatively smaller.

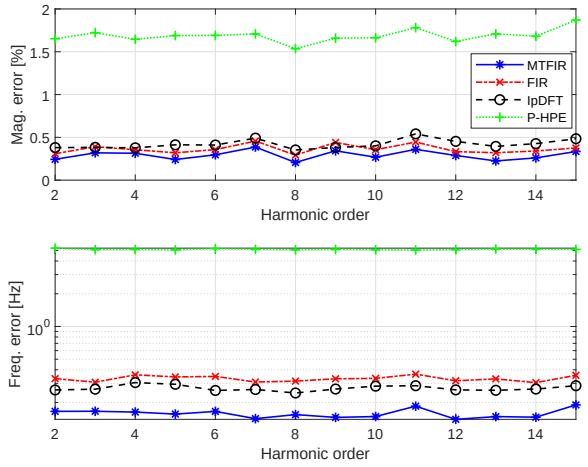

Fig. 9. Magnitude and frequency errors returned by the MTFIR filter, the conventional FIR filter, the IpDFT, and the P-HPE under joint interferences of noise, frequency deviation, and harmonic distortion.

F. Multiple Disturbances

In this section, we consider there are multiple disturbances mentioned earlier. Specifically, 80-dB wideband noise and a harmonic component are added to the signal (25). Also, the fundamental frequency has a deviation of 0.5 Hz, and the harmonic frequency is proportional to the fundamental one. The harmonic order, HFO frequency, and damping factor are the same with section V-C.

The corresponding results of the four estimators are shown in Fig. 9. We can see that even though there exist joint interferences of noise, frequency deviation, and harmonic distortion, the proposed MTFIR filter is still more accurate than the conventional FIR filter, the IpDFT, and the P-HPE in HFO magnitude and frequency estimation.

TABLE II
RESPONSE TIMES [MS] OF THE FOUR ESTIMATORS UNDER AMPLITUDE STEP CHANGE CONDITIONS. '-' MEANS THE CORRESPONDING RESULT IS NOT AVAILABLE.

HFO freq.	MTFIR	FIR	IpDFT	P-HPE
310 [Hz]	16.30	16.00	-	20.00
410 [Hz]	15.70	15.90	-	20.00
510 [Hz]	15.40	15.60	-	20.00
610 [Hz]	15.00	15.40	18.00	20.00
710 [Hz]	14.80	15.30	17.30	20.00
810 [Hz]	14.60	15.00	17.20	20.00
910 [Hz]	14.40	14.80	17.30	20.00
1010 [Hz]	14.20	14.60	17.00	20.00
1110 [Hz]	14.00	14.50	16.80	20.00
1210 [Hz]	13.90	14.30	16.40	20.00
1310 [Hz]	13.70	14.10	16.10	20.00
1410 [Hz]	13.60	14.10	16.00	20.00
1510 [Hz]	13.50	13.90	15.90	20.00
1610 [Hz]	13.40	13.70	15.70	20.00

TABLE III
RESPONSE TIMES [MS] OF THE THREE ESTIMATORS UNDER PHASE STEP CHANGE CONDITIONS. '-' HAS THE SAME MEANING AS IN TABLE II.

HFO freq.	MTFIR	FIR	IpDFT	P-HPE
310 [Hz]	14.40	14.10	-	19.30
410 [Hz]	13.80	14.00	-	19.30
510 [Hz]	13.40	13.60	-	19.40
610 [Hz]	12.90	13.10	17.40	19.40
710 [Hz]	12.30	12.60	16.20	19.40
810 [Hz]	12.00	12.30	15.60	19.40
910 [Hz]	11.70	11.90	15.70	19.40
1010 [Hz]	11.30	11.70	14.60	19.40
1110 [Hz]	11.00	11.30	14.70	19.40
1210 [Hz]	10.70	11.10	13.90	19.50
1310 [Hz]	10.50	10.80	13.60	19.50
1410 [Hz]	10.30	10.50	13.60	19.50
1510 [Hz]	10.10	10.30	13.10	19.50
1610 [Hz]	9.80	10.10	13.10	19.50

G. Step Change

To test the response performances of the three estimators in HFO phasor estimation, the signal (25) is used, where σ and f_1 is set at 0 and 50 Hz, respectively. Because there is no measurement standard for HFO parameter estimation, the response time defined in [8] is used to evaluate the response performance. The threshold for the total vector error is set to 1%. Please note that even under steady-state conditions, the frequency errors of the three estimators are always larger than the corresponding threshold (0.005 Hz). The response time in HFO frequency estimation is not available and not shown in this paper. In the amplitude step change test, when $t = 1$ s, the fundamental and HFO amplitudes change to 1.1 and 0.011, respectively. In the phase step change test, when $t = 1$ s, the initial phases of the fundamental and HFO components change to $\frac{\pi}{18}$ and $\frac{7\pi}{18}$ rad, respectively.

The response times of the four estimators under amplitude and phase step change conditions are shown in TABLE II and III, respectively. Please note that because the window length is different at different HFO frequencies, we show the results when f_i is from 310 Hz to 1610 Hz in a step of 100 Hz. We can see that the response times of the MTFIR filter under both step change conditions are always shorter than 20 ms, which can meet the corresponding requirement of the IEEE/IEC standard for P-class PMUs. Compared with the conventional FIR filter, the IpDFT, and the P-HPE, the response times of the MTFIR filter estimator are almost the same as the conventional FIR filter, and are shorter than those of the IpDFT and the P-HPE.

VI. COMPUTATION BURDEN

Because the optimal parameters of the MTFIR filter can be selected offline, the corresponding filter can be designed offline, and the main computations of the proposed estimator are in HFO phasor estimation. When the signal sampling frequency is 10 kHz, 402 real multiplications and 400 real additions are needed as the filter is 1-cycle-long. Such computations are very small and can be executed even by a cheap digital signal processor. Also, the computations of the conventional FIR filter, the P-HPE, and the IpDFT are the same with the proposed filter. With the consideration of the accuracy, response time, and computation burden performances of the three estimators, the proposed MTFIR filter is more applicable than the other three estimators.

VII. CONCLUSION

The multi-tone FIR (MTFIR) filter is proposed in this paper, and is truncated as an FIR filter for HFO magnitude and frequency estimation. The frequency error source of the proposed MTFIR filter is analyzed, and the optimal parameters of the MTFIR are selected based on the analysis results. Performance tests show that the proposed MTFIR filter is more accurate than the conventional FIR filter, the IpDFT, and the P-HPE in HFO magnitude and frequency estimation. The response time of the proposed estimator is shorter than 20 ms. In addition, the computation burden of the proposed estimator is very low. These performances make the proposed estimator suitable for HFO parameter estimation in practice.

REFERENCES

[1] C. Buchhagen, C. Rauscher, A. Menze, and J. Jung, "Borwin1 - first experiences with harmonic interactions in converter dominated grids," in *International ETG Congress 2015; Die Energiewende - Blueprints for the new energy age*, 2015, pp. 1–7.

[2] H. Saad, Y. Fillion, S. Deschanvres, Y. Vernay, and S. Dennetire, "On resonances and harmonics in hvdc-mmc station connected to ac grid," *IEEE Trans. Power Del.*, vol. 32, no. 3, pp. 1565–1573, 2017.

[3] C. Zou, H. Rao, S. Xu, and et al, "Analysis of resonance between a vsc-hvdc converter and the ac grid," *IEEE Trans. Power Electron.*, vol. 33, no. 12, pp. 10 157–10 168, 2018.

[4] J. Zhu, J. Hu, L. Lin, Y. Wang, and C. Wei, "High-frequency oscillation mechanism analysis and suppression method of vsc-hvdc," *IEEE Trans. Power Electron.*, vol. 35, no. 9, pp. 8892–8896, 2020.

[5] B. Pang, H. Nian, and Y. Xu, "Mechanism analysis and damping method for high frequency resonance between vsc-hvdc and the wind farm," *IEEE Trans. Energy Convers.*, vol. 36, no. 2, pp. 984–994, 2021.
[6] J. Man, L. Chen, V. Terzija, and X. Xie, "Mitigating high-frequency resonance in mmc-hvdc systems using adaptive notch filters," *IEEE Trans. Power Syst.*, pp. 1–1, 2021.
[7] Y. Ouyang, Z. Wang, G. Zhao, J. Hu, S. Ji, J. He, and S. X. Wang, "Current sensors based on gmr effect for smart grid applications," *Sensors and Actuators A: Physical*, vol. 294, pp. 8–16, 2019.
[8] "IEEE/IEC international standard - measuring relays and protection equipment - part 118-1: Synchrophasor for power systems - measurements," *IEC/IEEE 60255-118-1:2018*, pp. 1–78, 2018.
[9] J. Chen, X. Li, M. A. Mohamed, and T. Jin, "An adaptive matrix pencil algorithm based-wavelet soft-threshold denoising for analysis of low frequency oscillation in power systems," *IEEE Access*, vol. 8, pp. 7244–7255, 2020.
[10] J. Chen, T. Jin, M. A. Mohamed, and M. Wang, "An adaptive tls-esprit algorithm based on an s-g filter for analysis of low frequency oscillation in wide area measurement systems," *IEEE Access*, vol. 7, pp. 47 644–47 654, 2019.
[11] X. Yang, J. Zhang, X. Xie, and et al, "Interpolated DFT-based identification of sub-synchronous oscillation parameters using synchrophasor data," *IEEE Trans. Smart Grid*, vol. 11, no. 3, pp. 2662–2675, 2020.
[12] F. Zhang, L. Cheng, W. Gao, and R. Huang, "Synchrophasors-based identification for subsynchronous oscillations in power systems," *IEEE Trans. Smart Grid*, vol. 10, no. 2, pp. 2224–2233, 2019.
[13] Y. Ma, Q. Huang, Z. Zhang, and D. Cai, "Application of multisynchrosqueezing transform for subsynchronous oscillation detection using pmu data," *IEEE Trans. Ind. Appl.*, vol. 57, no. 3, pp. 2006–2013, 2021.
[14] L. Chen, W. Zhao, F. Wang, W. Qing, and H. Songling, "An interharmonic phasor and frequency estimator for subsynchronous oscillation identification and monitoring," *IEEE Trans. Instrum. Meas.*, vol. 68, no. 6, pp. 1714–1723, 2019.
[15] X. Xie, Y. Zhan, H. Liu, and C. Liu, "Improved synchrophasor measurement to capture sub/super-synchronous dynamics in power systems with renewable generation," *IET Renew. Power Gener.*, vol. 13, no. 1, pp. 49–56, 2019.
[16] J. Shair, X. Xie, L. Yuan, Y. Wang, and Y. Luo, "Monitoring of subsynchronous oscillation in a series-compensated wind power system using an adaptive extended kalman filter," *IET Renew. Power Gener.*, vol. 14, no. 19, pp. 4193–4203, 2020.
[17] B. Gao, R. Torquato, W. Xu, and W. Freitas, "Waveform-based method for fast and accurate identification of subsynchronous resonance events," *IEEE Trans. Power Syst.*, vol. 34, no. 5, pp. 3626–3636, 2019.
[18] H. Qian, R. Zhao, and T. Chen, "Interharmonics analysis based on interpolating windowed FFT algorithm," *IEEE Trans. Power Del.*, vol. 22, no. 2, pp. 1064–1069, 2007.
[19] P. Romano and M. Paolone, "Enhanced interpolated-DFT for synchrophasor estimation in fpgas: Theory, implementation, and validation of a pmu prototype," *IEEE Trans. Instrumen. Meas.*, vol. 63, no. 12, pp. 2824–2836, 2014.
[20] L. Chen, W. Zhao, F. Wang, and S. Huang, "Harmonic phasor estimator for p-class phasor measurement units," *IEEE Trans. Instrum. Meas.*, vol. 69, no. 4, pp. 1556–1565, 2020.
[21] K. Duda, T. P. Zieliski, A. Bie, and S. H. Barczentewicz, "Harmonic phasor estimation with flat-top fir filter," *IEEE Trans. Instrum. Meas.*, vol. 69, no. 5, pp. 2039–2047, 2020.
[22] C.-I. Chen and Y.-C. Chen, "Comparative study of harmonic and interharmonic estimation methods for stationary and time-varying signals," *IEEE Trans. Ind. Electron.*, vol. 61, no. 1, pp. 397–404, 2014.
[23] F. Harris, "On the use of windows for harmonic analysis with the discrete fourier transform," *Proc. IEEE*, vol. 66, no. 1, pp. 51–83, 1978.
[24] J. Man, X. Xie, S. Xu, C. Zou, and C. Yin, "Frequency-coupling impedance model based analysis of a high-frequency resonance incident in an actual mmc-hvdc system," *IEEE Trans. Power Del.*, vol. 35, no. 6, pp. 2963–2971, 2020.

Lei Chen (Member, IEEE) received the B.S. degree from North China Electric Power University, Baoding, China, in 2015. and the PhD degree from Tsinghua University, Beijing, China, both in electrical Engineering. He was a visiting PhD student with the University of California, Riverside, CA, US, in 2019.

His current research interests include phasor measurement unit algorithms, novel synchrophasor applications, and power system wideband oscillation analysis and control. He is a recipient of the *Best Dissertation Award* from Tsinghua University, Beijing, China.

Xiaorong Xie (Senior Member, IEEE) received the B.Sc. degree from Shanghai Jiao Tong University, Shanghai, China, in 1996, and the Ph.D. degree from Tsinghua University, Beijing, China, in 2001. He is currently a Full Professor with the Department of Electrical Engineering, Tsinghua University. His research interests include power system stability analysis and control, flexible ac transmission systems, and integration of renewables.